

Lamb wave propagation in elastic waveguides with variable thickness

BY VINCENT PAGNEUX^{1,*} AND AGNÈS MAUREL²

¹*Laboratoire d'Acoustique de l'Université du Maine, UMR CNRS 6613, Avenue Olivier Messiaen, 72085 Le Mans Cedex 9, France*

²*Laboratoire Ondes et Acoustique, UMR CNRS 7587, Ecole Supérieure de Physique et de Chimie Industrielles, 10 rue Vauquelin, 75005 Paris, France*

The problem of Lamb wave propagation in waveguides with varying height is treated by a multimodal approach. The technique is based on a rearrangement of the equations of elasticity that provides a new system of coupled mode equations preserving energy conservation. These coupled mode equations avoid the usual problem at the cut-offs with zero wavenumber. Thereafter, we define an impedance matrix that is governed by a Riccati equation yielding a stable numerical computation of the solution. Incidentally, the versatility of the multimodal method is exemplified by treating analytically the case of slowly varying guide and by showing how to get easily the Green tensor in any geometry. The method is applied for a waveguide whose height is described by a Gaussian function and the energy conservation is verified numerically. We determine the Green tensor in this geometry.

Keywords: elastic waveguide; impedance matrix; Lamb modes; multimodal method; varying height; scattering

1. Introduction

The interest in waves propagating in elastic waveguide comes, at least, from two applications. First in non-destructive testing, guided waves are believed to have a potential for improving inspection efficiency and sensitivity, compared with bulk-wave technique. Second in geophysics, they are the basic picture for seismic surface waves propagating in the crust and upper mantle.

To tackle the problem of waveguide thickness variation, different techniques have been proposed, such as hybrid boundary-element methods (Cho & Rose 1996; Cho 2000; Galan & Abascal 2003), finite-element methods (Koshiba *et al.* 1984; Galan & Abascal 2002; Wu *et al.* 2003) or modal methods (Abram 1974; Kennett 1984; Maupin 1988; Tromp 1994; Galanenko 1998; Folguera & Harris 1999). The modal approach offers the advantage of discretizing the transverse direction with transverse modes which implies, for instance, an exact solution for straight waveguide, and this method permits the reduction of the problem to an ordinary differential equation that governs the modal components resulting from the projection onto the modal basis.

* Author for correspondence (vincent.pagneux@univ-lemans.fr).

The problem of wave propagation in a two-dimensional waveguide can be formally written as an evolution problem $\partial_x \mathbf{z} = \mathcal{L} \mathbf{z}$, where x is the waveguide axis, $\mathbf{z} = (u, v, s, t)^T$ (u, v are the displacement components and $s \equiv \sigma_{xx}$, $t \equiv \sigma_{xy}$, with σ the stress tensor) and \mathcal{L} a differential operator. After \mathcal{L} has been diagonalized, this vector \mathbf{z} can be projected on the usual Lamb modes as $\mathbf{z} = \sum_n c_n \mathbf{z}_n$, where $\mathbf{z}_n = (\tilde{U}_n, \tilde{V}_n, \tilde{S}_n, \tilde{T}_n)^T$ satisfies the eigenvalue problem $\mathcal{L} \mathbf{z}_n = i k_n \mathbf{z}_n$. Then, using the biorthogonality relation satisfied by the eigenfunctions \mathbf{z}_n , the original evolution problem is thus reduced to a first-order ordinary differential equation on the components c_n (e.g. Maupin 1988).

There are two problems in this coupled mode method. The first problem concerns cut-offs that occur at isolated longitudinal coordinates x . At cut-offs, the eigenfunctions \mathbf{z}_n cannot form a base anymore. This problem is related to the normalization coefficient of the biorthogonality relation that vanishes at the cut-offs. It is also related to the impossibility to decompose \mathbf{z} into forward and backward modes at cut-offs. Relatively few works have been done to overcome this difficulty. Galanenko (1998) proposes to treat cut-offs by using the regular singularity theory of differential equation. The same kind of techniques has also been recently proposed by Perel *et al.* (2005). The second problem concerns the numerical implementation of the coupled mode equation which is not obvious. Indeed, the coupled mode equation corresponds to a boundary-value problem and the presence of evanescent modes makes the integration of the coupled mode equation numerically unstable if directly performed. To avoid this difficulty, Kennett (1984) used the technique of invariant embedding to obtain coupled Riccati equations on the reflection and transmission matrices.

In this paper, we propose a new formulation of the coupled mode method that is numerically stable and that partially solves the problem of cut-off (namely, the cut-offs with vanishing wavenumber k_n). Our formulation uses the symmetry properties of the Lamb modes between forward and backward modes. It permits one to decompose the two two-vectors $\mathbf{X} = (u, t)^T$, $\mathbf{Y} = (-s, v)^T$ into two biorthogonal bases $\tilde{\mathbf{X}}_n = (\tilde{U}_n, \tilde{T}_n)^T$, $\tilde{\mathbf{Y}}_n = (-\tilde{S}_n, \tilde{V}_n)^T$, which correspond to the forward modes only, instead of decomposing the four vector \mathbf{z} into both backward and forward modes. It is then possible to renormalize separately $\tilde{\mathbf{X}}_n$ and $\tilde{\mathbf{Y}}_n$, so that the renormalized \mathbf{X}_n and \mathbf{Y}_n remain bases at cut-offs with zero wavenumber. This gives two coupled evolution equations on a_n and b_n , the components of \mathbf{X} and \mathbf{Y} on the two renormalized bases. To avoid numerical instability, we define an impedance matrix \mathbf{Z} , which links the components through $\mathbf{b} = \mathbf{Z} \mathbf{a}$, and which is governed by a Riccati equation. This kind of technique has been used in the scalar case, where the impedance matrix is equivalent to a Dirichlet to Neumann operator (Pagneux *et al.* 1996). We could say that the matrix \mathbf{Z} for Lamb waves is an extension of the concept of the Dirichlet to Neumann operator to vector waves.

The rest of this paper is organized as follows. In §2, we present the derivation of the coupled equations. In §3, we define the impedance matrix and the Riccati equation. In §4, the energy conservation is discussed. In §5, some analytical solutions for slowly varying guides are presented. In §6, the derivation of the Green tensor in elastic waveguide is presented. Section 7 presents the numerical implementation that will be used to get the results of §8.

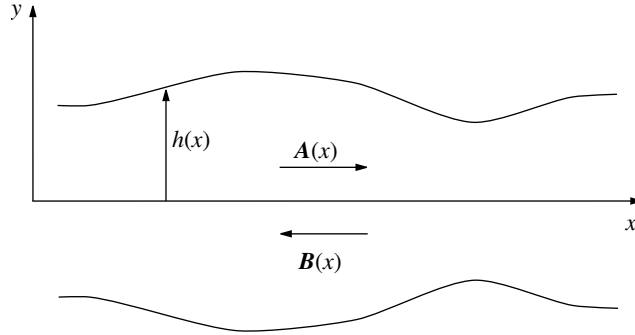


Figure 1. Geometry.

2. Coupled mode equations

In this section, the problem of guided wave is set using a modal expansion. The modal expansion we choose has been previously used in Pagneux & Maurel (2002, 2004). It is different from the coupled mode expansion classically used; indeed, one could think to write the problem as $\mathbf{z}' = \mathcal{L}\mathbf{z}$ (for instance, as in Maupin 1988), where $\mathbf{z} = (u, v, s, t)^T$ is a four-vector and to project on the usual Lamb modes $\mathbf{z}_n = (\tilde{U}_n, \tilde{V}_n, \tilde{S}_n, \tilde{T}_n)^T$ to obtain an evolution problem for the coefficient \mathbf{c} of \mathbf{z} . Instead, we choose to split the four-vector \mathbf{z} into two two-vectors $\mathbf{X} = (u, t)^T$, $\mathbf{Y} = (-s, v)^T$ and to perform the projection onto $\mathbf{X}_n = (U_n, T_n)^T$, $\mathbf{Y}_n = (-S_n, V_n)^T$, where \mathbf{X}_n , \mathbf{Y}_n are renormalized and build from the usual Lamb modes $\tilde{\mathbf{X}}_n$, $\tilde{\mathbf{Y}}_n$.

A first motivation to do that comes from Fraser’s biorthogonality relation (1976) $\int -\tilde{U}_n \tilde{S}_m + \tilde{T}_n \tilde{V}_m = \tilde{J}_n \delta_{nm}$ that simply translates into $(\tilde{\mathbf{X}}_n | \tilde{\mathbf{Y}}_m) = \tilde{J}_n \delta_{nm}$ when the form $(\mathbf{X} | \mathbf{Y}) \equiv \int -us + tv$ is defined. Also, the main motivation is to take care of the mode cut-offs (see for instance Perel *et al.* 2005), problems that are clearly translated to $\tilde{J}_n = 0$ in our formalism. In other words, the whole task in our formalism is to define the bases \mathbf{X}_n and \mathbf{Y}_n , from $\tilde{\mathbf{X}}_n$ and $\tilde{\mathbf{Y}}_n$, in a way such that $(\mathbf{X}_n | \mathbf{Y}_n) = J_n$ does not vanish at cut-offs. It is shown in the present work that this is possible for cut-offs with zero wavenumber. Finally, the problem is reduced to an evolution problem for the projection coefficients \mathbf{a} and \mathbf{b} of \mathbf{X} and \mathbf{Y} on the renormalized Lamb modes.

(a) Position of the problem

We are interested in the propagation of Lamb wave through a two-dimensional waveguide with a varying height, described by the function $h(x)$ (see figure 1), with free boundaries, and for which displacements are in the (x, y) plane (in-plane motion). For the sake of clarity, the waveguide is considered to be symmetric with respect to the horizontal axis, but the method can be easily extended to non-symmetric geometry $[h_1(x) \leq y \leq h_2(x)$ with $h_1(x) \neq -h_2(x)]$.

The time dependence is $e^{-i\omega\tau}$ and will be omitted in the following. The equation of motion is

$$-\rho\omega^2 \mathbf{w} = \nabla \cdot \boldsymbol{\sigma}, \tag{2.1}$$

where ρ is the density,

$$\mathbf{w} = \begin{pmatrix} u \\ v \end{pmatrix}$$

is the displacement vector and

$$\boldsymbol{\sigma} = \begin{pmatrix} s & t \\ t & r \end{pmatrix}$$

is the corresponding stress tensor, with

$$\left. \begin{aligned} s &= \lambda \partial_y v + (\lambda + 2\mu) \partial_x u, \\ t &= \mu (\partial_y u + \partial_x v), \\ r &= (\lambda + 2\mu) \partial_y v + \lambda \partial_x u, \end{aligned} \right\} \quad (2.2)$$

where (λ, μ) are the Lamé constants. The boundary condition at the faces $y = \pm h(x)$ are free of traction, corresponding to boundary conditions:

$$r[x, \pm h(x)] = \pm h'(x) t[x, \pm h(x)], \quad (2.3)$$

$$t[x, \pm h(x)] = \pm h'(x) s[x, \pm h(x)], \quad (2.4)$$

where $h'(x)$ is dh/dx .

(b) *Modal expansion*

It will be convenient to work on two quantities \mathbf{X} and \mathbf{Y} presented below. That formalism allows us to easily tackle the projection on the Lamb modes. The idea is to write the equations as an evolution equation (with respect to the coordinate x of the waveguide) on \mathbf{X} and \mathbf{Y} , which leads to a canonical eigenvalue problem in the transverse direction when transverse modes are sought. This formulation is similar to the one presented recently in Folguera & Harris (1999), in that it describes the evolution of a stress–displacement four-vector, but here that four-vector is suitably split into

$$\mathbf{X} = \begin{pmatrix} u \\ t \end{pmatrix} \quad \text{and} \quad \mathbf{Y} = \begin{pmatrix} -s \\ v \end{pmatrix}.$$

It is shown in appendix A that the elasticity equations (2.1)–(2.4) can be written as (see also Pagneux & Maurel 2004)

$$\partial_x \begin{pmatrix} \mathbf{X} \\ \mathbf{Y} \end{pmatrix} = \begin{pmatrix} 0 & \mathbf{F} \\ \mathbf{G} & 0 \end{pmatrix} \begin{pmatrix} \mathbf{X} \\ \mathbf{Y} \end{pmatrix}, \quad (2.5)$$

where \mathbf{F} and \mathbf{G} are the operator matrices:

$$\mathbf{F} = \begin{pmatrix} -\frac{f_1}{\lambda} & -f_1 \partial_y \\ f_1 \partial_y & -\rho \omega^2 - f_2 \partial_y^2 \end{pmatrix} \quad \text{and} \quad \mathbf{G} = \begin{pmatrix} \rho \omega^2 & \partial_y \\ -\partial_y & \frac{1}{\mu} \end{pmatrix}, \quad (2.6)$$

with $f_1 = \lambda/(\lambda + 2\mu)$ and $f_2 = 4\mu(\lambda + \mu)/(\lambda + 2\mu)$. Concerning the boundary conditions (2.4), since the problem is considered as an evolution equation (2.5) on \mathbf{X} and \mathbf{Y} , we always use the expressions of r written as a linear function of \mathbf{Y} , $r : \mathbf{Y} \rightarrow r(\mathbf{Y}) = f_1 s + f_2 \partial_y v$, which implies that the boundary conditions are entirely expressed in terms of \mathbf{X} and \mathbf{Y} .

Then, in order to project the evolution equation (2.5), we introduce the modes $(\tilde{\mathbf{X}}_n, \tilde{\mathbf{Y}}_n)^T$ solutions of the eigenvalue problem associated to (2.5),

$$ik_n \begin{pmatrix} \tilde{\mathbf{X}}_n \\ \tilde{\mathbf{Y}}_n \end{pmatrix} = \begin{pmatrix} 0 & \mathbf{F} \\ \mathbf{G} & 0 \end{pmatrix} \begin{pmatrix} \tilde{\mathbf{X}}_n \\ \tilde{\mathbf{Y}}_n \end{pmatrix}, \tag{2.7}$$

with boundary conditions $\tilde{r}_n = 0$ and $\tilde{t}_n = 0$ at $y = \pm h$. Equation (2.7) is a canonical eigenvalue problem, the solutions of which are the Lamb modes (see Viktorov 1967; Achenbach 1987). Assuming the completeness of the set of the Lamb modes (Kirrmann 1995; Besserer & Malishewsky 2004), the vector $(\mathbf{X}, \mathbf{Y})^T$ is expanded as

$$\begin{pmatrix} \mathbf{X} \\ \mathbf{Y} \end{pmatrix} = \sum_{n \neq 0} c_n \begin{pmatrix} \tilde{\mathbf{X}}_n \\ \tilde{\mathbf{Y}}_n \end{pmatrix}. \tag{2.8}$$

Here $n > 0$ refers to right-going mode and $n < 0$ refers to left-going modes. The eigenvalues k_n for right-going modes are sorted in ascending order of their imaginary part and descending order of their real part, and if k_n corresponds to a right-going mode, $-k_n$ corresponds to a left-going mode. As can be seen from equation (2.7), the symmetry properties of these bases impose $\tilde{\mathbf{X}}_{-n} = \pm \tilde{\mathbf{X}}_n$, $\tilde{\mathbf{Y}}_{-n} = \mp \tilde{\mathbf{Y}}_n$, and in the sequel we arbitrarily choose $\tilde{\mathbf{X}}_{-n} = -\tilde{\mathbf{X}}_n$, $\tilde{\mathbf{Y}}_{-n} = \tilde{\mathbf{Y}}_n$, as in Viktorov (1967). Owing to these symmetry properties, it is possible to write the decomposition (2.8) in term of the right-going modes only,

$$\mathbf{X} = \sum_{n > 0} \tilde{a}_n(x) \tilde{\mathbf{X}}_n(y), \quad \mathbf{Y} = \sum_{n > 0} \tilde{b}_n(x) \tilde{\mathbf{Y}}_n(y), \tag{2.9}$$

with $\tilde{a}_n = c_n - c_{-n}$ and $\tilde{b}_n = c_n + c_{-n}$.

For the projections, we use the inner product between two component functions that is defined by

$$\left(\begin{pmatrix} u_1 \\ v_1 \end{pmatrix} \middle| \begin{pmatrix} u_2 \\ v_2 \end{pmatrix} \right) = \int_{-h}^h (u_1 u_2 + v_1 v_2) dy.$$

Note that this inner product is not positive definite, since the vectors \mathbf{X} and \mathbf{Y} we are going to use are complex.

One advantage of our formalism (equation (2.5)) is that the operators \mathbf{F} and \mathbf{G} have the following remarkable properties (see appendix A):

$$\left. \begin{aligned} (\mathbf{F} \hat{\mathbf{Y}} | \mathbf{Y}) &= (\hat{\mathbf{Y}} | \mathbf{F} \mathbf{Y}) + [r \hat{v} - \hat{r} v]_{-h}^h, \\ (\mathbf{G} \hat{\mathbf{X}} | \mathbf{X}) &= (\hat{\mathbf{X}} | \mathbf{G} \mathbf{X}) + [u \hat{t} - \hat{u} t]_{-h}^h. \end{aligned} \right\} \tag{2.10}$$

That means that \mathbf{F} and \mathbf{G} are formally self-adjoint. In the particular case of the modes which have $r_n(\pm h) = 0$ and $t_n(\pm h) = 0$ and thus make the boundary terms vanish, the operators \mathbf{F} and \mathbf{G} are self-adjoint. Using the property of \mathbf{F} and \mathbf{G} (see (A 5)), we get $(\mathbf{F} \mathbf{G} \tilde{\mathbf{X}}_n | \tilde{\mathbf{Y}}_m) = (\tilde{\mathbf{X}}_n | \mathbf{G} \mathbf{F} \tilde{\mathbf{Y}}_m)$, that is $(k_m^2 - k_n^2)(\tilde{\mathbf{X}}_n | \tilde{\mathbf{Y}}_n) = 0$. This is

an easy way to derive the biorthogonality relation obtained by Fraser (1976): $(\tilde{\mathbf{X}}_n | \tilde{\mathbf{Y}}_m) = \tilde{J}_n \delta_{mn}$.

As could be anticipated, it appears that \tilde{J}_n vanishes for each mode cut-off that corresponds to coalescence of modes (Kirmann 1995). To avoid this latter problem for zero cut-offs ($k_n=0$), we choose to work with renormalized bases \mathbf{X}_n for \mathbf{X} and \mathbf{Y}_n for \mathbf{Y} built from $\tilde{\mathbf{X}}_n$ and $\tilde{\mathbf{Y}}_n$ in a way that is detailed in appendix B and where $(\mathbf{X}_n, Z_{c,n} \mathbf{Y}_n)^T$ is proportional to $(\tilde{\mathbf{X}}_n, \tilde{\mathbf{Y}}_n)^T$. Here, $Z_{c,n}$ appear as renormalization coefficients and correspond to the diagonal entries of the characteristic impedance matrix \mathbf{Z}_c (see §3). These new bases satisfy

$$ik_n \begin{pmatrix} \mathbf{X}_n \\ Z_{c,n} \mathbf{Y}_n \end{pmatrix} = \begin{pmatrix} 0 & \mathbf{F} \\ \mathbf{G} & 0 \end{pmatrix} \begin{pmatrix} \mathbf{X}_n \\ Z_{c,n} \mathbf{Y}_n \end{pmatrix}. \tag{2.11}$$

The modal decomposition is now done as

$$\begin{cases} \mathbf{X} = \sum_{n \in N} a_n(x) \mathbf{X}_n(y), \\ \mathbf{Y} = \sum_{n \in N} b_n(x) \mathbf{Y}_n(y), \end{cases} \quad \text{with } (\mathbf{X}_n | \mathbf{Y}_m) = J_n \delta_{mn} \tag{2.12}$$

(the expression of J_n is given in appendix C) and

$$\left. \begin{aligned} a_n &= a_n^+ + a_n^-, \\ b_n &= Z_{c,n}(a_n^+ - a_n^-). \end{aligned} \right\} \tag{2.13}$$

One important point is that \mathbf{X}_n and \mathbf{Y}_n remain bases for cut-offs with zero wavenumber ($k_n=0$).

(c) Evolution equation

The task is now to derive an evolution equation for the modal components $\mathbf{a}(x)$ and $\mathbf{b}(x)$. To do that, we project the system (2.5) on the bases $Z_{c,n} \mathbf{Y}_n$ and \mathbf{X}_n :

$$\begin{cases} (\partial_x \mathbf{X} | Z_{c,n} \mathbf{Y}_n) = (\mathbf{F} \mathbf{Y} | Z_{c,n} \mathbf{Y}_n), \\ (\partial_x \mathbf{Y} | \mathbf{X}_n) = (\mathbf{G} \mathbf{X} | \mathbf{X}_n). \end{cases} \tag{2.14}$$

Each term is then calculated using (2.12) and properties (A 4):

$$\begin{aligned} (\partial_x \mathbf{X} | Z_{c,n} \mathbf{Y}_n) &= Z_{c,n} (\partial_x \mathbf{X}_m | \mathbf{Y}_n) a_m + a'_n Z_{c,n} J_n \delta_{mn}, \\ (\mathbf{F} \mathbf{Y} | Z_{c,n} \mathbf{Y}_n) &= (\mathbf{Y} | \mathbf{F} Z_{c,n} \mathbf{Y}_n) + Z_{c,n} f_1 [v S_n - s V_n]_{-h}^h + Z_{c,n} f_2 [v \partial_y V_n - \partial_y v V_n]_{-h}^h \\ &= ik_n (\mathbf{Y} | \mathbf{X}_n) + [v R_n - r V_n]_{-h}^h = ik_n J_n b_m \delta_{mn}. \end{aligned}$$

Similarly,

$$\begin{aligned} (\partial_x \mathbf{Y} | \mathbf{X}_n) &= (\partial_x \mathbf{Y}_m | \mathbf{X}_n) b_m + b'_n J_n \delta_{mn}, \\ (\mathbf{G} \mathbf{X} | \mathbf{X}_n) &= (\mathbf{X} | \mathbf{G} \mathbf{X}_n) + [t U_n - T_n u]_{-h}^h = ik_n a_m Z_{c,n} J_n \delta_{mn} + [h' U_n S_m]_{-h}^h b_m. \end{aligned}$$

This leads to a system of first-order differential equations governing \mathbf{a} and \mathbf{b} :

$$\begin{cases} \mathbf{a}' = \mathbf{N}_1 \mathbf{a} + \mathbf{N}_2 \mathbf{b}, \\ \mathbf{b}' = \mathbf{N}_3 \mathbf{a} + \mathbf{N}_4 \mathbf{b}, \end{cases} \tag{2.15}$$

where matrices \mathbf{N}_1 to \mathbf{N}_4 are given by

$$\left. \begin{aligned} \mathbf{N}_1(n, m) &= -\frac{1}{J_n} (\partial_x X_m | Y_n), \\ \mathbf{N}_2(n, m) &= \frac{ik_n}{Z_{c,n}} \delta_{mn}, \\ \mathbf{N}_3(n, m) &= ik_n Z_{c,n} \delta_{mn}, \\ \mathbf{N}_4(n, m) &= \frac{1}{J_n} \{ -(\partial_x Y_m | X_n) + [h' U_n S_m]_{-h}^h \}. \end{aligned} \right\} \quad (2.16)$$

Expressions of matrices \mathbf{N}_1 and \mathbf{N}_4 , easier for numerical calculation, are given in appendix D.

3. The impedance matrix

In principle, equations (2.15) might be directly integrated, but there are two reasons that prevent one from doing that. First, the problem will be posed as a boundary-value problem with a radiation condition at the outlet of the waveguide and a source at the inlet, and the integration of (2.15) as an initial value problem would be very awkward. Second, the numerical integration of (2.15) appears to be unstable because of the presence of the evanescent modes that induce exponential growth (Pagneux *et al.* 1996). In order to circumvent these two problems, it has been proven to be useful to define the impedance matrix \mathbf{Z} (Pagneux *et al.* 1996) as the linear operator that links together vectors $\mathbf{a}(x)$ and $\mathbf{b}(x)$ at a given x position,

$$\mathbf{b}(x) = \mathbf{Z}(x)\mathbf{a}(x). \quad (3.1)$$

Using the definition of the impedance matrix $\mathbf{Z}(x)$, it is easily obtained from (2.15) that $\mathbf{Z}(x)$ obeys a Riccati matrix differential equation,

$$\mathbf{Z}'(x) = \mathbf{N}_3 + \mathbf{N}_4\mathbf{Z}(x) - \mathbf{Z}(x)\mathbf{N}_1 - \mathbf{Z}(x)\mathbf{N}_2\mathbf{Z}(x). \quad (3.2)$$

This allows us to solve the problem of guided wave in any configuration by simply solving the Riccati differential equation on \mathbf{Z} , starting from a radiation condition at the outlet, e.g. at the guide terminations, with either $\mathbf{a}^+ = 0$ or $\mathbf{a}^- = 0$, we get $\mathbf{Z} = \pm \mathbf{Z}_c$, where \mathbf{Z}_c is the so-called characteristic impedance matrix which is diagonal with entries $Z_{c,n}$.

Once \mathbf{Z} has been calculated, the whole fields can be obtained by integrating

$$\mathbf{a}'(x) = [\mathbf{N}_1 + \mathbf{N}_2\mathbf{Z}(x)]\mathbf{a}(x), \quad (3.3)$$

obtained from equation (2.15) and where the source imposes \mathbf{a}^+ at the inlet. The successive integrations of equations (3.2) and (3.3) are numerically stable, even in the presence of evanescent modes.

(a) Reflection and transmission matrices

If the interest is in the determination of the elastic fields between the inlet and the outlet, one has to integrate successively the above equations (3.2) and (3.3), but this necessitates storing the \mathbf{Z} matrix at each point x during the first

integration (3.2) to perform the second integration (3.3). On the other hand, if the interest is only in the scattering matrix, i.e. the knowledge of the reflection matrix \mathbf{R} and the transmission matrix \mathbf{T} , this storage is not necessary, as shown below.

To determine \mathbf{R} , which is defined at the inlet abscissa x_{ini} by

$$\mathbf{a}^-(x_{\text{ini}}) = \mathbf{R}\mathbf{a}^+(x_{\text{ini}}), \quad (3.4)$$

it is sufficient to know $\mathbf{Z}(x_{\text{ini}})$, since \mathbf{R} is related to $\mathbf{Z}(x_{\text{ini}})$ through

$$\mathbf{R} = [\mathbf{Z}_c + \mathbf{Z}(x_{\text{ini}})]^{-1}[\mathbf{Z}_c - \mathbf{Z}(x_{\text{ini}})], \quad (3.5)$$

easily obtained from equations (2.13).

To determine \mathbf{T} , we define the matrix \mathbf{Y} as the operator that links together the coefficients \mathbf{a} between the outlet abscissa x_f and any $x \leq x_f$ through

$$\mathbf{a}(x_f) = \mathbf{Y}(x_f, x)\mathbf{a}(x). \quad (3.6)$$

Note that \mathbf{Y} corresponds to the propagator of equation (3.3). Then, by differentiating equation (3.6) with respect to x , we get the following differential equation governing \mathbf{Y} :

$$\mathbf{Y}' = -\mathbf{Y}[\mathbf{N}_1 + \mathbf{N}_2\mathbf{Z}], \quad (3.7)$$

that has to be integrated from $x=x_f$ to $x=x_{\text{ini}}$ with the initial condition $\mathbf{Y}(x_f, x=x_f) = \mathbf{I}$. The transmission matrix \mathbf{T} is defined by

$$\mathbf{a}^+(x_f) = \mathbf{T}\mathbf{a}^+(x_{\text{ini}}), \quad (3.8)$$

and is related to the matrix \mathbf{Y} through

$$\mathbf{T} = \mathbf{Y}(x_f, x_{\text{ini}})[\mathbf{I} + \mathbf{R}]. \quad (3.9)$$

Eventually, to obtain matrices \mathbf{R} and \mathbf{T} , it is sufficient to integrate the coupled equations (3.2) and (3.7) from $x=x_f$ to $x=x_{\text{ini}}$ and this without storing any matrix.

4. Energy flux conservation

In this section, we want to verify that the coupled mode equations conserve the energy flux. At each x position, the energy flux W is defined by $W(x) = \int_S \langle \boldsymbol{\pi} \rangle d\mathbf{S}$, where the average is taken over time and where $\boldsymbol{\pi} = \sigma(\dot{u}, \dot{v})^T$ is the Poynting vector (overdot indicates the time derivative). In the harmonic regime, we get

$$W(x) = \frac{\omega}{2} \text{Im}[(\mathbf{X} | \bar{\mathbf{Y}})], \quad (4.1)$$

where the overbar means complex conjugation. Introducing the matrix $\mathbf{K}_{mn} = (\mathbf{X}_m | \bar{\mathbf{Y}}_n)$, the energy flux can be expressed as $W(x) = (\omega/2) \text{Im}[\mathbf{a}^T \mathbf{K} \bar{\mathbf{b}}]$. It is sufficient to use the properties: $k_n \rightarrow \bar{k}_n$ gives $\mathbf{X}_n \rightarrow \bar{\mathbf{X}}_n$, $\mathbf{Y}_n \rightarrow \bar{\mathbf{Y}}_n$ and $k_n \rightarrow -k_n$ gives $\mathbf{X}_n \rightarrow \mathbf{X}_n$, $\mathbf{Y}_n \rightarrow \mathbf{Y}_n$, to build the matrix \mathbf{M} , such as $\bar{\mathbf{X}}_n = \mathbf{M}_{nm} \mathbf{X}_m$ and $\bar{\mathbf{Y}}_n = \mathbf{M}_{nm} \mathbf{Y}_m$: for real and imaginary k_n values ($k_n = \pm \bar{k}_n$), we get $\bar{\mathbf{X}}_n$ and $\bar{\mathbf{Y}}_n$ real, so \mathbf{M} locally equals identity; for k_n complex, say $n=2$, we consider $k_3 = -\bar{k}_2$, so $\mathbf{X}_3 = \bar{\mathbf{X}}_2$, $\mathbf{Y}_3 = \bar{\mathbf{Y}}_2$, and we get locally \mathbf{M} equals

$$\begin{pmatrix} 0 & 1 \\ 1 & 0 \end{pmatrix}.$$

With $\mathbf{J}_{mn} = (\mathbf{X}_m | \mathbf{Y}_n)$, we thus get $\mathbf{K} = \mathbf{J}\mathbf{M}$ (\mathbf{M} equals its transpose, with $\mathbf{M}^2 = \mathbf{I}$) and the final expression of the flux,

$$W(x) = \frac{\omega}{2} \text{Im}[\mathbf{a}^T \mathbf{J}\mathbf{M}\bar{\mathbf{b}}]. \tag{4.2}$$

(a) Energy conservation

Let us calculate $W' = dW/dx$,

$$W' = \text{Im}[(\mathbf{J}\mathbf{a}')^T \mathbf{M}\bar{\mathbf{b}} + \mathbf{a}^T \mathbf{M}\overline{\mathbf{J}\mathbf{b}'} + \mathbf{a}^T \mathbf{J}'\mathbf{M}\bar{\mathbf{b}}], \tag{4.3}$$

using $\mathbf{J}\mathbf{M} = \mathbf{M}\bar{\mathbf{J}}$. We now write the system (2.15) as

$$\left. \begin{aligned} \mathbf{J}\mathbf{a}' &= \mathbf{M}_1 \mathbf{a} + \mathbf{D}(ikJ/Z_c) \mathbf{b}, \\ \mathbf{J}\mathbf{b}' &= \mathbf{D}(ikJZ_c) \mathbf{a} + \mathbf{M}_4 \mathbf{b}, \end{aligned} \right\} \tag{4.4}$$

where $\mathbf{D}(a)$ denotes the diagonal matrix with a_n as n th diagonal elements and $\mathbf{M}_1(n, m) = -(\partial_x X_m | Y_n)$, $\mathbf{M}_4(n, m) = -(\partial_x Y_m | X_n) + [h' U_n S_m]_{-h}^h$. By differentiating the biorthogonality relation in (2.12), it is easy to check that

$$\mathbf{J}' = -\mathbf{M}_1^T - \mathbf{M}_4. \tag{4.5}$$

Also, $\overline{\mathbf{M}}_{1mn} = -(\partial_x \bar{X}_m | \bar{Y}_n) = \mathbf{M}_{ml}(\partial_x X_l | Y_k) \mathbf{M}_{kn}$, so $\overline{\mathbf{M}}_1 = \mathbf{M}\mathbf{M}_1\mathbf{M}$ and, as well

$$\overline{\mathbf{M}}_4 = \mathbf{M}\mathbf{M}_4\mathbf{M}. \tag{4.6}$$

We get, using equations (4.4) and (4.5),

$$W' = \text{Im}[\mathbf{b}^T \mathbf{D}(ikJ/Z_c) \mathbf{M}\bar{\mathbf{b}} + \mathbf{a}^T \mathbf{M}\mathbf{D}(\overline{ikJZ_c}) \bar{\mathbf{a}}] + \text{Im}[\mathbf{a}^T (\mathbf{M}\overline{\mathbf{M}}_4 - \mathbf{M}_4\mathbf{M}) \bar{\mathbf{b}}]. \tag{4.7}$$

The matrix $(\mathbf{M}\overline{\mathbf{M}}_4 - \mathbf{M}_4\mathbf{M})$ equal zero because of property (4.6) with $\mathbf{M}^2 = \mathbf{I}$. The two first quantities of the right-hand side term also equal zero: for k_n real or imaginary, both $ik_n J_n / Z_{c,n}$ and $\overline{ik_n J_n Z_{c,n}}$ are real; for k_n complex, say $n=2$, it is sufficient to consider $k_3 = -\bar{k}_2$ (and $J_3 = \bar{J}_2$, $Z_{c,3} = \bar{Z}_{c,2}$) to check that $\mathbf{b}^T \mathbf{D}(ikJ/Z_c)^T \mathbf{M}\bar{\mathbf{b}}$ is equal to

$$i \begin{pmatrix} b_2 & b_3 \end{pmatrix} \begin{pmatrix} 0 & k_2 J_2 / Z_{c,2} \\ -\overline{k_2 J_2 / Z_{c,2}} & 0 \end{pmatrix} \begin{pmatrix} \bar{b}_2 \\ \bar{b}_3 \end{pmatrix} = i(k_2 J_2 / Z_{c,2} b_2 \bar{b}_3 - cc),$$

(cc denotes the complex conjugate), with zero imaginary part.

We finally obtain $W' = 0$, which shows that the system is written in a form that implies energy conservation.

(b) Reflection and transmission coefficients

To define the fraction of reflected/transmitted energy, the energy flux is written as

$$\begin{aligned} W &= \text{Im}[(\mathbf{a}^+ + \mathbf{a}^-)^T \mathbf{K}\bar{\mathbf{Z}}_c(\overline{\mathbf{a}^+} - \overline{\mathbf{a}^-})] \\ &= \text{Im}[(\mathbf{a}^+)^T \mathbf{J}\mathbf{M}\bar{\mathbf{Z}}_c \overline{\mathbf{a}^+} - (\mathbf{a}^-)^T \mathbf{J}\mathbf{M}\bar{\mathbf{Z}}_c \overline{\mathbf{a}^-}] + \text{Im}[(\mathbf{a}^-)^T \mathbf{J}\mathbf{M}\bar{\mathbf{Z}}_c \overline{\mathbf{a}^+} - (\mathbf{a}^+)^T \mathbf{J}\mathbf{M}\bar{\mathbf{Z}}_c \overline{\mathbf{a}^-}]. \end{aligned} \tag{4.8}$$

The structure of matrix $\mathbf{JM}\bar{\mathbf{Z}}_c$ is as follows: for k_n real, it locally equals $J_n\bar{\mathbf{Z}}_{c,n} = -J_nZ_{c,n} \in i\mathbf{R}$. For imaginary k_n value, it locally equals $J_n\bar{\mathbf{Z}}_{c,n} = J_nZ_{c,n} \in \mathbf{R}$. For two complex conjugate, say $k_3 = -\bar{k}_2$, we get locally,

$$\begin{pmatrix} 0 & J_2\bar{\mathbf{Z}}_{c,3} \\ J_3\bar{\mathbf{Z}}_{c,2} & 0 \end{pmatrix} = \begin{pmatrix} 0 & J_2Z_{c,2} \\ \overline{J_2Z_{c,2}} & 0 \end{pmatrix}.$$

Consequently, both terms of the right-hand side term in equation (4.8) can be written as

$$\begin{aligned} \text{Im}[(\mathbf{a}^+)^T \mathbf{JM}\bar{\mathbf{Z}}_c \overline{\mathbf{a}^+} - (\mathbf{a}^-)^T \mathbf{JM}\bar{\mathbf{Z}}_c \overline{\mathbf{a}^-}] &= \sum_{k_n \in \mathbf{R}} iJ_nZ_{c,n}|a_n^+|^2 - \sum_{k_n \in \mathbf{R}} iJ_nZ_{c,n}|a_n^-|^2, \\ \text{Im}[(\mathbf{a}^-)^T \mathbf{JM}\bar{\mathbf{Z}}_c \overline{\mathbf{a}^+} - (\mathbf{a}^+)^T \mathbf{JM}\bar{\mathbf{Z}}_c \overline{\mathbf{a}^-}] &= 2 \sum_{k_n \in i\mathbf{R}} J_nZ_{c,n} \text{Im}(a_n^+ \overline{a_n^-}) \\ &\quad + 2 \sum_{k_{n+1} = -\bar{k}_n} \text{Im}[J_nZ_{c,n}(a_n^+ \overline{a_{n+1}^-} - \overline{a_n^-} a_{n+1}^+)]. \end{aligned}$$

The first term accounts for the energy flux carried by the propagating modes, while the second terms account for the energy flux carried by evanescent modes.

Let us consider the case where N propagating modes are sent at the waveguide inlet $x = x_i$, that is $\mathbf{a}(x_i) = (a_1, \dots, a_N, 0, \dots, 0)^T$ and a radiation condition at the waveguide outlet $x = x_o$, that is $\mathbf{a}^-(x_o) = \mathbf{0}$. We get

$$\left. \begin{aligned} W(x_i) &= \sum_{n=1}^N iJ_nZ_{c,n}|a_n^+(x_i)|^2 - \sum_{n=1}^N iJ_nZ_{c,n}|a_n^-(x_i)|^2, \\ W(x_o) &= \sum_{n=1}^{N'} iJ_nZ_{c,n}|a_n^+(x_o)|^2, \end{aligned} \right\} \quad (4.9)$$

where N' denotes the number of propagating modes at $x = x_o$ ($N' \neq N$ a priori if $h(x_o)$ differs from $h(x_i)$). The energy conservation implies $W(x_i) = W(x_o)$ and we define the coefficients of reflected energy F_R and transmitted energy $F_T = 1 - F_R$,

$$F_R = \frac{\sum_{n=1}^N J_nZ_{c,n}|a_n^-(x_i)|^2}{\sum_{n=1}^N J_nZ_{c,n}|a_n^+(x_i)|^2}, \quad F_T = \frac{\sum_{n=1}^{N'} J_nZ_{c,n}|a_n^+(x_o)|^2}{\sum_{n=1}^N J_nZ_{c,n}|a_n^+(x_i)|^2}. \quad (4.10)$$

5. Analytical solutions for slowly varying guides

We present here the WKB (Wentzel–Kramer–Brillouin) approximation of equation (2.5) by using the biorthogonality relation (2.12). This approximation is valid for a slowly varying waveguide. The height h is supposed to vary slowly and we denote $\zeta = \epsilon x$ the slow variable, where ϵ measures the slowness. The following WKB ansatz is proposed for the four-vector (as in Folguera & Harris 1999),

$$\begin{pmatrix} \mathbf{X} \\ \mathbf{Y} \end{pmatrix} = \exp[i\varphi(\zeta)/\epsilon] \sum_{\nu \geq 0} \epsilon^\nu \begin{pmatrix} \mathbf{X}^\nu \\ \mathbf{Y}^\nu \end{pmatrix}. \quad (5.1)$$

In the following, we denote

$$\mathbf{X}^\nu = \begin{pmatrix} u^\nu \\ t^\nu \end{pmatrix} \quad \text{and} \quad \mathbf{Y}^\nu = \begin{pmatrix} -s^\nu \\ v^\nu \end{pmatrix},$$

and $r^\nu = f_1 s^\nu + f_2 \partial_y v^\nu$. We insert (5.1) in equation (2.5). At zero order in ϵ , we obtain

$$[\mathcal{L} - i\phi'(\zeta)] \begin{pmatrix} \mathbf{X}^0 \\ \mathbf{Y}^0 \end{pmatrix} = 0, \tag{5.2}$$

where

$$\mathcal{L} = \begin{pmatrix} 0 & \mathbf{F} \\ \mathbf{G} & 0 \end{pmatrix},$$

and with the boundary conditions $r^0 = t^0 = 0$. We thus deduce that $(\mathbf{X}^0, \mathbf{Y}^0)^T$ and ϕ' are, respectively, an eigenvector and an eigenvalue of the eigenvalue problem (2.7) for a given mode number n ,

$$\phi'(\zeta) = k_n, \tag{5.3}$$

and

$$\begin{pmatrix} \mathbf{X}^0 \\ \mathbf{Y}^0 \end{pmatrix} = \alpha_n \begin{pmatrix} \mathbf{X}_n \\ Z_{c,n} \mathbf{Y}_n \end{pmatrix}, \tag{5.4}$$

where the proportionality factor α_n will be determined by the equation at first order. First order in ϵ leads to

$$(\mathbf{M} - ik_n) \begin{pmatrix} \mathbf{X}^1 \\ \mathbf{Y}^1 \end{pmatrix} = \partial_\zeta \begin{pmatrix} \mathbf{X}^0 \\ \mathbf{Y}^0 \end{pmatrix}, \tag{5.5}$$

with boundary conditions $t^1 = h' s^0$ and $r^1 = 0$. Equation (5.5) and the associated boundary conditions determine the evolution law for α_n . Equation (5.5) is projected on the four-vector

$$\begin{pmatrix} Z_{c,n} \mathbf{Y}_n \\ \mathbf{X}_n \end{pmatrix},$$

$$\begin{aligned} & (\mathbf{F} \mathbf{Y}^1 | Z_{c,n} \mathbf{Y}_n) + (\mathbf{G} \mathbf{X}^1 | \mathbf{X}_n) - ik_n [(\mathbf{X}^1 | Z_{c,n} \mathbf{Y}_n) + (\mathbf{Y}^1 | \mathbf{X}_n)] \\ & = (\partial_\zeta \mathbf{X}^0 | Z_{c,n} \mathbf{Y}_n) + (\partial_\zeta \mathbf{Y}^0 | \mathbf{X}_n). \end{aligned} \tag{5.6}$$

Properties (A 4) give $(\mathbf{F} \mathbf{Y}^1 | Z_{c,n} \mathbf{Y}_n) = (\mathbf{Y}^1 | \mathbf{F} Z_{c,n} \mathbf{Y}_n) + [Z_{c,n} V_n r^1 + Z_{c,n} R_n v^1]_{-h}^h = ik_n (\mathbf{Y}^1 | \mathbf{X}_n)$ and $(\mathbf{G} \mathbf{X}^1 | \mathbf{X}_n) = (\mathbf{X}^1 | \mathbf{G} \mathbf{X}_n) + [U_n t^1 - T_n u^1]_{-h}^h = ik_n (\mathbf{X}^1 | \mathbf{Y}_n) + [h' s^0 U_n]_{-h}^h$. We thus obtain

$$[h' s^0 U_n]_{-h}^h = (\partial_\zeta \mathbf{X}^0 | Z_{c,n} \mathbf{Y}_n) + (\partial_\zeta \mathbf{Y}^0 | \mathbf{X}_n),$$

and using equation (5.4)

$$2\alpha'_n Z_{c,n} J_n + \alpha_n \{ (\partial_\zeta \mathbf{X}_n | Z_{c,n} \mathbf{Y}_n) + (\mathbf{X}_n | \partial_\zeta (Z_{c,n} \mathbf{Y}_n)) - Z_{c,n} [h' U_n S_n]_{-h}^h \} = 0. \tag{5.7}$$

With $J'_n = (\partial_\zeta \mathbf{X}_n | \mathbf{Y}_n) + (\mathbf{X}_n | \partial_\zeta \mathbf{Y}_n) - [h' U_n S_n]_{-h}^h$, we get

$$2\alpha'_n Z_{c,n} J_n + \alpha_n (Z_{c,n} J'_n + Z'_{c,n} J_n) = 0. \tag{5.8}$$

Assuming α_n non-zero, equation (5.8) is equivalent to

$$\partial_\zeta (\alpha_n^2 Z_{c,n} J_n) = 0. \tag{5.9}$$

Eventually, the WKB solution is

$$\begin{pmatrix} \mathbf{X} \\ \mathbf{Y} \end{pmatrix} = \alpha_n \exp[i\varphi(\zeta)/\epsilon] \begin{pmatrix} \mathbf{X}_n \\ Z_{c,n} \mathbf{Y}_n \end{pmatrix}, \tag{5.10}$$

with φ and α_n determined by equations (5.3) and (5.9). Obviously, this WKB solution shows no coupling between modes and it conserves the energy.

6. Green tensor

To get the usual Green tensor G_{ij} ($i=1, 2$), giving the displacements from a delta function force, we start from

$$-\rho\omega^2 G_{ij}(\mathbf{r}, \mathbf{r}') + L_{ik} G_{kj}(\mathbf{r}, \mathbf{r}') = \delta_{ij} \delta(\mathbf{r} - \mathbf{r}'), \tag{6.1}$$

where $\mathbf{r}=(x, y)$ is the vector position. If $\mathbf{u}=(u_1=u, u_2=v)$ denotes the displacement fields satisfying

$$-\rho\omega^2 u_i(\mathbf{r}) + L_{ik} u_k(\mathbf{r}) = f_i, \tag{6.2}$$

where $\mathbf{f} = (F_1, F_2)^T \delta(\mathbf{r} - \mathbf{r}_0)$ is a delta function force located in \mathbf{r}_0 , we have

$$u_i(\mathbf{r}) = \int d\mathbf{r}' G_{ik}(\mathbf{r}, \mathbf{r}') f_k(\mathbf{r}') = F_1 G_{i1}(\mathbf{r}, \mathbf{r}_0) + F_2 G_{i2}(\mathbf{r}, \mathbf{r}_0). \tag{6.3}$$

As a consequence, the four components of the Green tensor can be simply deduced through the displacement fields

$$\mathbf{u}(\mathbf{r}) = \begin{pmatrix} G_{11}(\mathbf{r}, \mathbf{r}_0) \\ G_{21}(\mathbf{r}, \mathbf{r}_0) \end{pmatrix}, \quad \text{for } F_2 = 0 \quad \text{and} \quad \mathbf{u}(\mathbf{r}) = \begin{pmatrix} G_{12}(\mathbf{r}, \mathbf{r}_0) \\ G_{22}(\mathbf{r}, \mathbf{r}_0) \end{pmatrix}, \quad \text{for } F_1 = 0. \tag{6.4}$$

In our formalism, equation (6.2) becomes, from equation (2.5),

$$\partial_x \begin{pmatrix} \mathbf{X} \\ \mathbf{Y} \end{pmatrix} = \begin{pmatrix} 0 & \mathbf{F} \\ \mathbf{G} & 0 \end{pmatrix} \begin{pmatrix} \mathbf{X} \\ \mathbf{Y} \end{pmatrix} + \begin{pmatrix} 0 \\ -F_2 \\ F_1 \\ 0 \end{pmatrix} \delta(\mathbf{r} - \mathbf{r}_0). \tag{6.5}$$

Integrating equation (6.5) w.r.t. x between $x_0 - \epsilon$ and $x_0 + \epsilon$, it is easy to see that $\llbracket u \rrbracket = \llbracket v \rrbracket = 0$, $\llbracket t \rrbracket = -F_2 \delta(y - y_0)$ and $\llbracket -s \rrbracket = F_1 \delta(y - y_0)$ (where $\llbracket z(x) \rrbracket = \lim_{\epsilon \rightarrow 0} z(x_0 + \epsilon) - z(x_0 - \epsilon)$).

We then project $\llbracket X \rrbracket = \sum_m \llbracket a_m \rrbracket X_m$ on Y_n , with

$$\llbracket X \rrbracket = \begin{pmatrix} 0 \\ -F_2 \delta(y - y_0) \end{pmatrix},$$

and $\llbracket Y \rrbracket = \sum_m \llbracket b_m \rrbracket Y_m$ on X_n , with

$$\llbracket Y \rrbracket = \begin{pmatrix} F_1 \delta(y - y_0) \\ 0 \end{pmatrix},$$

to get

$$\llbracket a_n \rrbracket = -F_2 \frac{V_n(y_0)}{J_n}, \quad \llbracket b_n \rrbracket = F_1 \frac{U_n(y_0)}{J_n}. \tag{6.6}$$

For the sake of simplicity and without loss of generality, we choose $x_0 = 0$ in the following. The numerical resolution can be now solved using $Z(L^+) = Z_c$ at the waveguide exit and calculating $Z(x)$ from L^+ to $x = 0^+$, as described in §8b. Similarly, $Z(x < 0)$ is calculated integrating from $Z(-L^-) = -Z_c$ to $x = 0^-$. The source is taken into account at $x = 0$ with

$$\left. \begin{aligned} \mathbf{a}(0^+) &= [Z(0^-) - Z(0^+)]^{-1} (Z(0^-) \llbracket \mathbf{a} \rrbracket - \llbracket \mathbf{b} \rrbracket), & \text{and } \mathbf{b}(0^+) &= Z(0^+) \mathbf{a}(0^+), \\ \mathbf{a}(0^-) &= [Z(0^-) - Z(0^+)]^{-1} (Z(0^+) \llbracket \mathbf{a} \rrbracket - \llbracket \mathbf{b} \rrbracket), & \text{and } \mathbf{b}(0^-) &= Z(0^-) \mathbf{a}(0^-), \end{aligned} \right\} \tag{6.7}$$

where $\llbracket \mathbf{a} \rrbracket = (\llbracket a_n \rrbracket)$ and $\llbracket \mathbf{b} \rrbracket = (\llbracket b_n \rrbracket)$ are given in equations (6.6). From these initial conditions on \mathbf{a} and \mathbf{b} at $x = 0^\pm$, we can calculate $\mathbf{a}(x)$ and $\mathbf{b}(x)$ until $x = \pm L^\pm$ (and thus the corresponding displacement fields).

(a) Green tensor of a straight waveguide

In the case of a straight waveguide (h constant), the calculation can be done explicitly, since we simply have $a_n(x) = a_n(0^+) e^{ik_n x}$ and $b_n(x) = b_n(0^+) e^{ik_n x}$, for $x > 0$, $a_n(x) = a_n(0^-) e^{-ik_n x}$ and $b_n(x) = b_n(0^-) e^{-ik_n x}$, for $x < 0$. With $Z(0^\pm) = \pm Z_c$, we get

$$\left. \begin{aligned} \mathbf{a}(0^+) &= \frac{1}{2} (\llbracket \mathbf{a} \rrbracket + Z_c^{-1} \llbracket \mathbf{b} \rrbracket), & \text{and } \mathbf{b}(0^+) &= \frac{1}{2} (Z_c \llbracket \mathbf{a} \rrbracket + \llbracket \mathbf{b} \rrbracket), \\ \mathbf{a}(0^-) &= -\frac{1}{2} (\llbracket \mathbf{a} \rrbracket - Z_c^{-1} \llbracket \mathbf{b} \rrbracket), & \text{and } \mathbf{b}(0^-) &= \frac{1}{2} (Z_c \llbracket \mathbf{a} \rrbracket - \llbracket \mathbf{b} \rrbracket). \end{aligned} \right\} \tag{6.8}$$

Using equations (6.4) and (6.6)–(6.8), we obtain

$$\left. \begin{aligned} G_{11}(\mathbf{r}, \mathbf{r}_0) &= \sum_{n>0} \frac{1}{2Z_{c,n}J_n} U_n(y_0) U_n(y) e^{ik_n|x|}, \\ G_{21}(\mathbf{r}, \mathbf{r}_0) &= \text{sign}(x) \sum_{n>0} \frac{1}{2J_n} U_n(y_0) V_n(y) e^{ik_n|x|}, \\ G_{12}(\mathbf{r}, \mathbf{r}_0) &= -\text{sign}(x) \sum_{n>0} \frac{1}{2J_n} V_n(y_0) U_n(y) e^{ik_n|x|}, \\ G_{22}(\mathbf{r}, \mathbf{r}_0) &= -\sum_{n>0} \frac{Z_{c,n}}{2J_n} V_n(y_0) V_n(y) e^{ik_n|x|}. \end{aligned} \right\} \tag{6.9}$$

These expressions are identical to those found by Karhitonov (1978). Note also that at $x=0$, the quantities $\sum_n (1/J_n) U_n(y_0) V_n(y)$ and $\sum_n (1/J_n) V_n(y_0) U_n(y)$ defining G_{12} and G_{21} vanish, as does any series with terms $(1/J_n) (\int dy f(y) V_n(y)) U_n(y)$ or $(1/J_n) (\int dy f(y) U_n(y)) V_n(y)$ for a given function f . Here, this means, for instance, that a force applied along the y -direction does not produce any displacement along the x -direction (this could also be deduced simply by symmetry argument, for instance the symmetry $x \rightarrow -x$ for G_{12}).

7. Numerical resolution

To solve a typical problem in a waveguide, namely with a radiation condition and a source, one has to solve first the Riccati equation (3.2) and, second, equation (3.3). By integrating equation (3.3), $\mathbf{a}(x)$ and $\mathbf{b}(x) = \mathbf{Z}(x)\mathbf{a}(x)$ are known in the whole space and, thus, the stress and displacement fields also.

We propose two numerical resolutions of equations (3.2) and (3.3). One resolution method uses a Magnus method for both equations and is detailed below. This method has three advantages: (i) it gives an exact solution for straight waveguide, (ii) the step size is not imposed by the wavelength, but rather by the typical variation length of the waveguide, (iii) it is not sensitive to the quasi-resonances that may be displayed by the behaviour of the impedance (Schiff & Shnider 1999). However, this Magnus method is not adapted to pass through cut-offs with non-zero wavenumber.

The other resolution method is used when cut-off has to be taken into account. In that case, we add a small dissipation to transform the singularity into quasi-singularity at cut-off. Nevertheless, passing through this quasi-singularity requires a smaller step size and is more time-consuming. This resolution, that uses two classical integration schemes, is not detailed below. To integrate the equation (3.2), we use a classical Runge–Kutta scheme with adaptative step size. The details of the scheme are not developed here and can be found in Press *et al.* (1993) for instance. Then, $\mathbf{a}(x_i)$ is then simply calculated solving equation (3.3) using a classical Crank–Nicholson scheme, well adapted to preserve the energy conservation.

(a) Magnus method

Our scheme is inspired by the techniques proposed by Schiff & Shnider (1999) and Iserles *et al.* (1999). The radiation condition gives \mathbf{Z} at x_f and the source \mathbf{a} is imposed at x_{ini} (figure 2). Then the interval $[x_{\text{ini}}; x_f]$ is discretized with dx step, so $x_n = x_{\text{ini}} + n dx$ and a second set $X_n = x_n + dx/2$ is defined.

If we start from equation (2.15), the Magnus method gives

$$\begin{pmatrix} \mathbf{a}(x_{n+1}) \\ \mathbf{b}(x_{n+1}) \end{pmatrix} = \begin{pmatrix} \mathbf{E}_1(X_n) & \mathbf{E}_2(X_n) \\ \mathbf{E}_3(X_n) & \mathbf{E}_4(X_n) \end{pmatrix} \begin{pmatrix} \mathbf{a}(x_n) \\ \mathbf{b}(x_n) \end{pmatrix}, \quad (7.1)$$

with matrix

$$\mathbf{N}(X_n) = \begin{pmatrix} \mathbf{N}_1(X_n) & \mathbf{N}_2(X_n) \\ \mathbf{N}_3(X_n) & \mathbf{N}_4(X_n) \end{pmatrix},$$

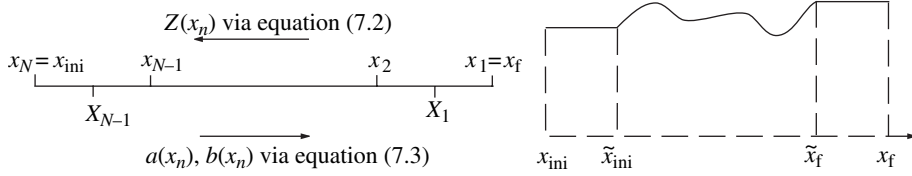


Figure 2. Discretization along the axis of the waveguide.

and matrices \mathbf{E}_1 to \mathbf{E}_4 defined by

$$\exp(-\mathbf{N} dx) = \begin{pmatrix} \mathbf{E}_1(X_n) & \mathbf{E}_2(X_n) \\ \mathbf{E}_3(X_n) & \mathbf{E}_4(X_n) \end{pmatrix},$$

(calculated at X_n midpoint between x_n and x_{n+1}), and that eventually permits one to obtain the following scheme for \mathbf{Z} :

$$\mathbf{Z}(x_{n+1}) = [\mathbf{E}_3(X_n) + \mathbf{E}_4(X_n)\mathbf{Z}(x_n)][\mathbf{E}_1(X_n) + \mathbf{E}_2(X_n)\mathbf{Z}(x_n)]^{-1}, \quad (7.2)$$

with $\mathbf{Z}(x_1) = \mathbf{Z}_c$. Note that integration is performed from right to left.

Then, equation (7.1) is used once again to get

$$\mathbf{a}(x_n) = [\mathbf{E}_1(X_n) + \mathbf{E}_2(X_n)\mathbf{Z}(x_n)]^{-1}\mathbf{a}(x_{n+1}), \quad (7.3)$$

where the calculation is done from left to right, starting from $\mathbf{a}(x_N)$.

(b) Calculation in the inlet/outlet portion with constant cross-section

When the waveguide begin or ends with a portion of constant cross-section, the displacement field can be determined analytically. Suppose that the portion with varying cross-section corresponds to $\tilde{x}_{ini} < x < \tilde{x}_f$ (figure 2). In this portion, the fields are numerically calculated, using either a Runge–Kutta scheme or matrix exponential. To obtain the field between x_{ini} and \tilde{x}_{ini} (waveguide inlet) and the field between \tilde{x}_f and x_f (waveguide outlet), we use:

- (i) For the waveguide outlet, $\tilde{x}_f \leq x \leq x_f$, $a_n(x) = a_n(\tilde{x}_f)e^{ik_n(x-\tilde{x}_f)}$ for both symmetric and antisymmetric modes, with no left-going modes. $a_n(\tilde{x}_f)$ is known from the numerical calculation between \tilde{x}_{ini} and \tilde{x}_f .
- (ii) For the waveguide inlet, $x_{ini} \leq x \leq \tilde{x}_{ini}$, we have $\mathbf{a}(x) = [\mathbf{I} + \mathbf{R}(\tilde{x}_{ini})]\mathbf{a}^+(x)$, with $a_n^+(x) = a_n^+(x_{ini})e^{ik_n(x-x_{ini})}$ that accounts for the incident wave at x_{ini} . Again, $\mathbf{R}(\tilde{x}_{ini})$ is known from the numerical calculation between \tilde{x}_{ini} and \tilde{x}_f .

8. Results

We report in this section results obtained with our method. The spectrum for Lamb modes is determined using the spectral method described in Pagneux & Maurel (2001), with a relative accuracy of 10^{-9} . The material constituting the waveguide has the following properties: Poisson ratio $s = 0.31$, $c_t = 2/\pi$, $c_l = 2/\pi\sqrt{2(1-s)/(1-2s)}$ and $\rho = 1$.

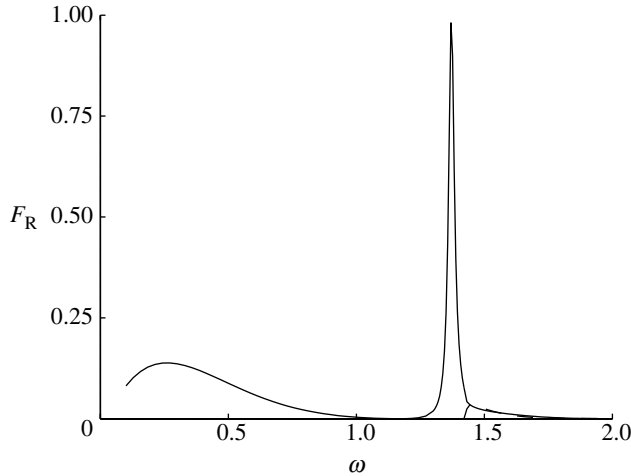


Figure 3. Coefficient of energy reflection F_R as a function of the frequency ω .

(a) *Reflection in a non-uniform guide*

We consider here the calculation of the coefficient of energy reflection and transmission. The geometry consists of a waveguide whose cross-section is described by a Gaussian function,

$$h(x) = h_0 + (h_1 - h_0)\exp\left(-\frac{x^2}{L^2}\right), \quad (8.1)$$

with $h_0 = 0.7$, $h_1 = 1.5$ and $L = 1.5$.

The incident wave at $x = -3L$ contains only the first antisymmetric mode A_0 and the geometry being symmetric with respect to $y = 0$, only antisymmetric modes are considered. The range for ω is such that for $\omega < 0.65$, only A_0 is propagating in the whole waveguide. For $0.65 < \omega < 1.42$, the mode A_1 is evanescent for h_0 and propagating for h_1 . Finally, for $1.42 < \omega < 2$, both modes A_0 and A_1 are propagating in the whole waveguide. The calculation is performed using matrix exponential with $N_m^{AS} = 11$ and 170 steps in the whole range of considered frequencies.

Figure 3 shows the variation of the coefficient of energy reflection F_R as a function of the frequency ω . The energy conservation relation $F_R + F_T = 1$ is satisfied in the whole range of frequency with an accuracy of around 10^{-5} .

The curve in plain line corresponds to the energy ratio transported by the mode A_0 , always propagating. At the cut-off frequency $\omega \approx 1.42$, the mode A_1 becomes propagating and, therefore, transports a part of the energy (curve in dotted line). Finally, at frequency $\omega \approx 1.37$, F_R reaches a maximum very close the value 1. This behaviour indicates that this frequency corresponds to a quasi-trapped mode, whose shape is indicated in figure 4b.

(b) *Green tensor*

We focus here on the Green tensor in a waveguide whose cross-section is described by the Gaussian function, as in §8a, with $h_0 = 1$, $h_1 = 1.4$, $L = 1$. The frequency is $\omega = 5$. For h_0 , there are four symmetric and five antisymmetric

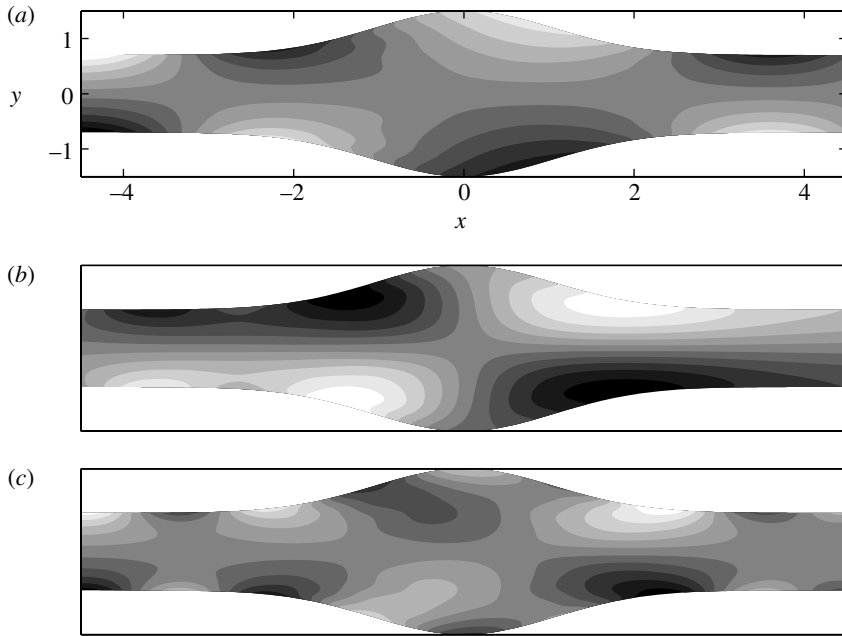


Figure 4. u -displacement fields for (a) $\omega=0.5$, (b) $\omega=1.37$ and (c) $\omega=1.5$.

propagating modes and for h_1 , there are six symmetric modes and six antisymmetric propagating modes.

Since there are cut-offs with non-zero wavenumber in this configuration, the numerical calculation is performed using the Runge–Kutta scheme with a relative tolerance of 10^{-6} . The source point being located at $(0, h_0/2)$, the calculations are divided into two parts, between 0 and x_f and between 0 and x_{ini} , using the initial conditions of equations (6.7), as described in §6

With $N_m^{AS} = 41$ and $N_m^S = 40$, the Runge–Kutta calculation needs $N=1500$ and 750 steps (respectively for antisymmetric and symmetric modes) for the calculation in the right part and $N=300$ and 350 steps for the calculations in the left part.

The displacement fields obtained are shown in figure 5. Note that we observe wiggles at the vertical of the source point, characteristic of the modal decomposition of the Green tensor. This calculation has been performed with an imaginary part ϵ of the frequency equal to 10^{-2} in order to avoid the cut-offs with non-zero wavenumber. The value of ϵ is small enough not to influence the final result, as shown in figure 6.

9. Closing remarks

The method developed in this paper is a multimodal method for waveguide with height variation. The two main advantages of this method are: (i) it avoids singularities at cut-offs with zero wavenumber and (ii) it can be implemented without numerical instability owing to the introduced impedance matrix. The way to avoid singularities at cut-offs with non-zero wavenumber remains an open question.

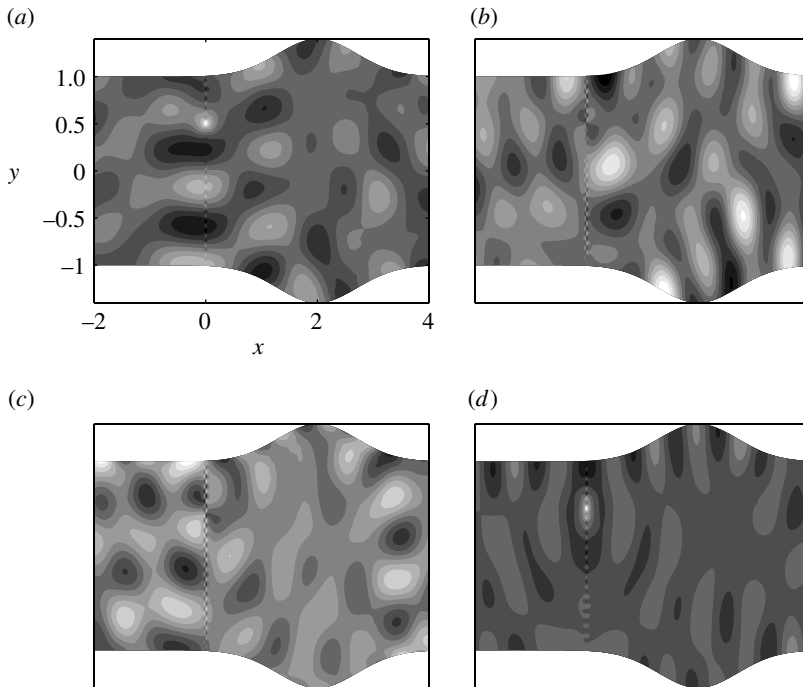


Figure 5. Green tensor for a source point located at $(0, h_0/2)$. Real part of the u -displacement fields associated with the Green tensor (a) G_{11} , (b) G_{21} , (c) G_{12} and (d) G_{22} for $\epsilon = 10^{-2}$.

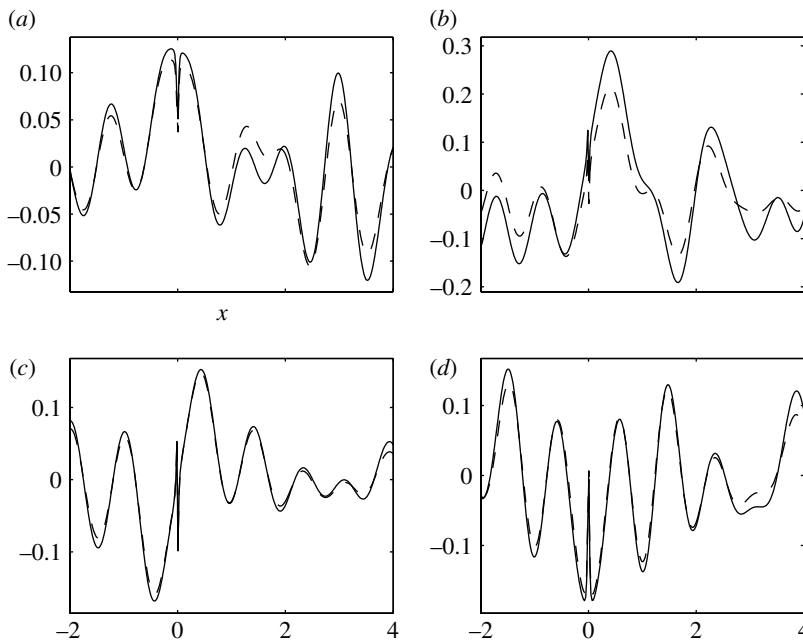


Figure 6. Profiles of the u -displacement at $y=0$ for $\epsilon = 10^3$ (solid line) and $\epsilon = 10^{-2}$ (dotted line).

We think that it is a valuable alternative to purely numerical methods, e.g. the finite-element method or the boundary-element method, because it allows both the brute force numerical calculation and the asymptotic approximation analysis.

Appendix A

(a) Derivation of the differential system

The derivation of equation (2.5) from equations (2.1)–(2.4) is as follow. The first step consists to obtain r as a function of (u, v, s, t) . This is done using its definition, that is the third equation of (2.2), that is written as $r = f_1 s + f_2 \partial_y v$, where $f_1 = \lambda/(\lambda + 2\mu)$ and $f_2 = (4\mu(\lambda + \mu))/(\lambda + 2\mu)$. Then, equation (2.5) can be written as

$$\left. \begin{aligned} -\rho\omega^2 u &= \partial_x s + \partial_y t, \\ -\rho\omega^2 v &= \partial_x t + \partial_y r = \partial_x t + f_1 \partial_y s + f_2 \partial_y^2 v. \end{aligned} \right\} \tag{A 1}$$

The definitions of s and t (first and second equations of (2.2)) give

$$\left. \begin{aligned} s &= \lambda \partial_y v + (\lambda + 2\mu) \partial_x u = \lambda(\partial_y v + \partial_x u/f_1), \\ t &= \mu(\partial_y u + \partial_x v). \end{aligned} \right\} \tag{A 2}$$

From (A 1) and (A 2), it is now straightforward to obtain

$$\left. \begin{aligned} \partial_x \mathbf{X} &= \begin{pmatrix} \partial_x u \\ \partial_x t \end{pmatrix} = \begin{pmatrix} \frac{f_1}{\lambda} s - f_1 \partial_y v \\ -\rho\omega^2 v - f_1 \partial_y s - f_2 \partial_y^2 v \end{pmatrix}, \\ \partial_x \mathbf{Y} &= \begin{pmatrix} -\partial_x s \\ \partial_x v \end{pmatrix} = \begin{pmatrix} \rho\omega^2 u + \partial_y t \\ \frac{1}{\mu} t - \partial_y u \end{pmatrix}. \end{aligned} \right\} \tag{A 3}$$

(b) Properties of matrices \mathbf{F} and \mathbf{G}

We give here properties of \mathbf{F} and \mathbf{G} for two vectors $\mathbf{Z}_1 = (z_{11}, z_{12})^T$ and $\mathbf{Z}_2 = (z_{21}, z_{22})^T$:

$$\left. \begin{aligned} (\mathbf{FZ}_1 | \mathbf{Z}_2) &= (\mathbf{Z}_1 | \mathbf{FZ}_2) + f_1 [z_{11} z_{22} - z_{12} z_{21}]_{-h}^h + f_2 [z_{12} \partial_y z_{22} - \partial_y z_{12} z_{22}]_{-h}^h, \\ (\mathbf{GZ}_1 | \mathbf{Z}_2) &= (\mathbf{Z}_1 | \mathbf{GZ}_2) + [z_{12} z_{21} - z_{11} z_{22}]_{-h}^h. \end{aligned} \right\} \tag{A 4}$$

Using (A 4), it is easy to also obtain

$$\begin{aligned}
 (\mathbf{FGZ}_1|\mathbf{Z}_2) &= (\mathbf{Z}_1|\mathbf{GFZ}_2) + f_1[(\mathbf{GZ}_1)_1 z_{22} - (\mathbf{GZ}_1)_2 z_{21}]^h_{-h} + f_2[(\mathbf{GZ}_1)_2 \partial_y z_{22} \\
 &\quad - \partial_y (\mathbf{GZ}_1)_2 z_{22}]^h_{-h} + [z_{12}(\mathbf{FZ}_2)_1 - z_{11}(\mathbf{FZ}_2)_2]^h_{-h}.
 \end{aligned}
 \tag{A 5}$$

Appendix B. Renormalization of the bases $\tilde{\mathbf{X}}_n$ and $\tilde{\mathbf{Y}}_n$

In this appendix, we show how to construct the renormalized bases \mathbf{X}_n and \mathbf{Y}_n from the usual bases $\tilde{\mathbf{X}}_n$ and $\tilde{\mathbf{Y}}_n$, in order that \mathbf{X}_n and \mathbf{Y}_n remain the basis for zero cut-offs ($k_n=0$).

Looking for a solution in $e^{ik_n x}$ leads to search A_n and B_n , in

$$\left. \begin{aligned}
 \phi_n(x, y) &= A_n \cosh(\beta_n y), \\
 \psi_n(x, y) &= B_n \sinh(\alpha_n y)/\alpha_n,
 \end{aligned} \right\} \text{for symmetric modes,}$$

$$\left. \begin{aligned}
 \phi_n(x, y) &= A_n \sinh(\beta_n y)/\beta_n, \\
 \psi_n(x, y) &= B_n \cosh(\alpha_n y),
 \end{aligned} \right\} \text{for antisymmetric modes.}$$
(B 1)

where the scalar potential ϕ_n and potential vector $(0, 0, \psi_n)$ define

$$\left. \begin{aligned}
 u_n &= ik_n \phi_n + \partial_y \psi_n, \\
 v_n &= \partial_y \phi_n - ik_n \psi_n, \\
 s_n/\mu &= -(k_n^2 + 2\beta_n^2 - \alpha_n^2)\phi_n + 2ik_n \partial_y \psi_n, \\
 t_n/\mu &= 2ik_n \partial_y \phi_n + (k_n^2 + \alpha_n^2)\psi_n.
 \end{aligned} \right\}$$
(B 2)

This is with $\alpha_n = (k_n^2 - k_t^2)^{1/2}$, $\beta_n = (k_n^2 - k_l^2)^{1/2}$, $k_t = \omega/c_t = (\rho/\mu)^{1/2}\omega$ and $k_l = \omega/c_l = (\rho/(\lambda + 2\mu))^{1/2}\omega$. To ensure the solution satisfies the boundary condition $r_n = t_n = 0$, A_n and B_n must satisfy

$$\mathbf{M} \begin{pmatrix} A_n \\ B_n \end{pmatrix} = 0,$$
(B 3)

with

$$\left. \begin{aligned}
 \mathbf{M} &= \begin{pmatrix} (k_n^2 + \alpha_n^2)\cosh(\beta_n h) & -2ik_n \cosh(\alpha_n h) \\ 2ik_n \alpha_n \beta_n \sinh(\beta_n h) & (k_n^2 + \alpha_n^2)\sinh(\alpha_n h) \end{pmatrix}, \\
 &\quad \text{for symmetric modes,} \\
 &= \begin{pmatrix} (k_n^2 + \alpha_n^2)\sinh(\beta_n h) & -2ik_n \alpha_n \beta_n \sinh(\alpha_n h) \\ 2ik_n \cosh(\beta_n h) & (k_n^2 + \alpha_n^2)\cosh(\alpha_n h) \end{pmatrix}, \\
 &\quad \text{for antisymmetric modes.}
 \end{aligned} \right\}$$
(B 4)

The dispersion relations $D(k, \omega) = 0$ (Viktorov 1967) is $\det(\mathbf{M}) = 0$,

$$D(k, \omega) = \begin{cases} (k^2 + \alpha^2)^2 \sinh(\alpha h) \cosh(\beta h) / \alpha - 4k^2 \beta \sinh(\beta h) \cosh(\alpha h), \\ \text{for symmetric modes,} \\ (k^2 + \alpha^2)^2 \sinh(\beta h) \cosh(\alpha h) / \beta - 4k^2 \alpha \sinh(\alpha h) \cosh(\beta h), \\ \text{for antisymmetric modes.} \end{cases} \quad (\text{B } 5)$$

In our formalism, the vanishing of one of the two vectors $\tilde{\mathbf{X}}_n = (\tilde{U}_n, \tilde{T}_n)^T$ or $\tilde{\mathbf{Y}}_n = (-\tilde{S}_n, \tilde{V}_n)^T$ is not acceptable. We have to ensure that this does not occur. In order to see how the vanishing of these modes may occur we write them as follows:

$$\begin{aligned} \tilde{\mathbf{X}}_n &= ik_n A_n \begin{pmatrix} \cosh(\beta_n y) \\ 2\mu \beta_n \sinh(\beta_n y) \end{pmatrix} + B_n \begin{pmatrix} \cosh(\alpha_n y) \\ \mu(k_n^2 + \alpha_n^2) \sinh(\alpha_n y) / \alpha_n \end{pmatrix}, \\ \tilde{\mathbf{Y}}_n &= ik_n B_n \begin{pmatrix} -2\mu \cosh(\alpha_n y) \\ -\sinh(\alpha_n y) / \alpha_n \end{pmatrix} + A_n \begin{pmatrix} \mu(k_n^2 + 2\beta_n^2 - \alpha_n^2) \cosh(\beta_n y) \\ \beta_n \sinh(\beta_n y) \end{pmatrix}, \end{aligned}$$

for symmetric modes and

$$\begin{aligned} \tilde{\mathbf{X}}_n &= ik_n A_n \begin{pmatrix} \sinh(\beta_n y) / \beta_n \\ 2\mu \cosh(\beta_n y) \end{pmatrix} + B_n \begin{pmatrix} \alpha_n \sinh(\alpha_n y) \\ \mu(k_n^2 + \alpha_n^2) \cosh(\alpha_n y) \end{pmatrix}, \\ \tilde{\mathbf{Y}}_n &= ik_n B_n \begin{pmatrix} -2\mu \alpha_n \sinh(\alpha_n y) \\ -\cosh(\alpha_n y) \end{pmatrix} + A_n \begin{pmatrix} \mu(k_n^2 + 2\beta_n^2 - \alpha_n^2) \sinh(\beta_n y) / \beta_n \\ \cosh(\beta_n y) \end{pmatrix}, \end{aligned}$$

for antisymmetric modes.

For $k_n = 0$, some care has to be taken when either (i) for symmetric modes, $\cosh(\beta_n h) \simeq k_n^2$ (for antisymmetric modes, $\sinh(\beta_n h) \simeq k_n^2$) or (ii) for symmetric modes, $\sinh(\alpha_n h) \simeq k_n^2$ (for antisymmetric modes, $\cosh(\alpha_n h) \simeq k_n^2$). In fact, configuration (i) corresponds to a pure longitudinal mode and makes the $\tilde{\mathbf{X}}_n$ vanish ($B_n = 0$) and configuration (ii) corresponds to a pure transverse mode and makes $\tilde{\mathbf{Y}}_n$ vanish ($A_n = 0$). Then, it is sufficient to renormalize the modes by dividing $\tilde{\mathbf{X}}_n$ by B_n and $\tilde{\mathbf{Y}}_n$ by A_n to avoid the vanishing of the modes at $k_n = 0$. A last step in the renormalization of the modes is needed because of the Lamé modes, where for symmetric modes $(\alpha_n^2 + k_n^2) \simeq \cosh(\alpha_n h)$ vanishes (for antisymmetric modes, $(\alpha_n^2 + k_n^2) \simeq \sinh(\alpha_n h)$ vanishes). For Lamé modes, the ratio B_n/A_n diverges and this necessitates a new renormalization of the modes $\tilde{\mathbf{Y}}_n$, where this ratio would appear, by multiplying it by $(\alpha_n^2 + k_n^2)$.

Eventually the renormalized bases will be defined by $\mathbf{X}_n = \tilde{\mathbf{X}}_n/B_n$ and $\mathbf{Y}_n = \tilde{\mathbf{Y}}_n(\alpha_n^2 + k_n^2)/A_n$.

With $Z_{c,n} = A_n/[B_n(\alpha_n^2 + k_n^2)]$ whose expression is deduced from (B 3),

$$\left. \begin{aligned} Z_{c,n} &= -\frac{\sinh(\alpha_n h)}{2ik_n \alpha_n \beta_n \sinh(\beta_n h)} = \frac{2ik_n \cosh(\alpha_n h)}{(\alpha_n^2 + k_n^2)^2 \cosh(\beta_n h)}, \\ &\text{for symmetric modes,} \\ &= -\frac{\cosh(\alpha_n h)}{2ik_n \cosh(\beta_n h)} = \frac{2ik_n \alpha_n \beta_n \sinh(\alpha_n h)}{(\alpha_n^2 + k_n^2)^2 \sinh(\beta_n h)}, \\ &\text{for antisymmetric modes,} \end{aligned} \right\} \quad (\text{B } 6)$$

we get, for symmetric modes,

$$\left. \begin{aligned} U_n &= ik_n(\alpha_n^2 + k_n^2)Z_{c,n} \cosh(\beta_n y) + \cosh(\alpha_n y), \\ V_n &= (\alpha_n^2 + k_n^2)\beta_n \sinh(\beta_n y) - ik_n/Z_{c,n} \sinh(\alpha_n y)/\alpha_n, \\ S_n/\mu &= -(\alpha_n^2 + k_n^2)(k_n^2 + 2\beta_n^2 - \alpha_n^2)\cosh(\beta_n y) + 2ik_n/Z_{c,n} \cosh(\alpha_n y), \\ T_n/\mu &= 2ik_n\beta_n(\alpha_n^2 + k_n^2)Z_{c,n} \sinh(\beta_n y) + (\alpha_n^2 + k_n^2)\sinh(\alpha_n y)/\alpha_n, \end{aligned} \right\} \quad (\text{B } 7)$$

and for antisymmetric modes,

$$\left. \begin{aligned} U_n &= ik_n(\alpha_n^2 + k_n^2)Z_{c,n} \sinh(\beta_n y)/\beta_n + \alpha_n \sinh(\alpha_n y), \\ V_n &= (\alpha_n^2 + k_n^2)\cosh(\beta_n y) - ik_n/Z_{c,n} \cosh(\alpha_n y), \\ S_n/\mu &= -(\alpha_n^2 + k_n^2)(k_n^2 + 2\beta_n^2 - \alpha_n^2)\sinh(\beta_n y)/\beta_n + 2ik_n\alpha_n/Z_{c,n} \sinh(\alpha_n y), \\ T_n/\mu &= 2ik_n\beta_n(\alpha_n^2 + k_n^2)Z_{c,n} \cosh(\beta_n y) + (\alpha_n^2 + k_n^2)\cosh(\alpha_n y). \end{aligned} \right\}$$

The two renormalized sets of vectors $\mathbf{X}_n = (U_n, T_n)^T$ and $\mathbf{Y}_n = (-S_n, V_n)^T$ continue to verify the biorthogonality condition and permit to project the elastic fields for ‘zero-coalescence’ of the mode wavenumbers $k_n=0$. Note also that vectors \mathbf{X}_n and \mathbf{Y}_n offer the advantage of being even functions of a_n , β_n and k_n , and, consequently, they have no branch points.

It has to be stressed that this useful renormalization of Lamb modes has been done owing to the formalism presented in this paper, i.e. the splitting of the original four-vector $(u, v, s, t)^T$ into two two-vectors $(u, t)^T$ and $(-s, v)^T$.

A problem that we have not resolved remains in the choice of these two bases: when two modes associated to wavenumbers k_m and $k_{m+1} (= -\overline{k_m})$ coalesce on the imaginary axis or when two modes associated to wavenumbers k_m and $-\overline{k_{m+1}} (= \overline{k_m})$ coalesce on the real axis, the two vectors, although both non-zero, are orthogonal and the method of projection fails (J_n vanishes).

Appendix C. Biorthogonality relation and expression of J_n

The biorthogonality condition (Fraser 1976; Murphy & Li 1994) for an in-plane problem can be written as: $(\mathbf{x}_n | \mathbf{y}_m) = \int (-u_n s_m + v_m t_n) dy = j_n \delta_{nm}$. With

$J_n = (\mathbf{X}_n | \mathbf{Y}_n) = j_n(\alpha_n^2 + k_n^2)/(A_n B_n)$ and using the dispersion relations, we get

$$J_n = i\mu \frac{k_n}{Z_{c,n}} \left\{ \sinh(2\alpha_n h) P(k_n) \pm (k_n^2 - \alpha_n^2) \left[1 - \frac{\alpha_n \sinh(2\alpha_n h)}{\beta_n \sinh(2\beta_n h)} \right] \right\}, \quad (C 1)$$

where ‘ \pm ’ indicates ‘+’ for symmetric modes and ‘-’ for antisymmetric modes, and where $P(k_n) = -\alpha_n(k_n^2 - \alpha_n^2)/(2\beta_n^2) + \alpha_n^3/k_n^2 - k_n^2/(2\alpha_n) + 3.5/\alpha_n - 8\alpha_n^3/(k_n^2 + \alpha_n^2)$.

Appendix D. Expression of matrices \mathbf{N}_i

$$\mathbf{N}_1(n, m) = \begin{cases} -\frac{1}{4J_n} \left\{ 2J'_n + 2J_n \frac{Z'_{c,n}}{Z_{c,n}} + \left[h' \left\{ U_n S_n + i\rho\omega^2 \left(\frac{U_n^2}{k_n Z_{c,n}} + \frac{Z_{c,n} V_n^2}{k_n} \right) \right\} \right]_{-h}^h \right\}, & \text{for } m = n, \\ \frac{1}{(k_m^2 - k_n^2) J_n} \left[h' \left\{ -k_m^2 U_m S_n + i\rho\omega^2 \left(\frac{k_n U_n U_m}{Z_{c,n}} - k_m Z_{c,m} V_n V_m \right) \right\} \right]_{-h}^h, & \text{for } m \neq n, \end{cases} \quad (D 1)$$

$$\mathbf{N}_4(n, m) = \begin{cases} \frac{1}{4J_n} \left\{ -2J'_n + 2J_n \frac{Z'_{c,n}}{Z_{c,n}} + \left[h' \left\{ U_n S_n + i\rho\omega^2 \left(\frac{U_n^2}{k_n Z_{c,n}} + \frac{Z_{c,n} V_n^2}{k_n} \right) \right\} \right]_{-h}^h \right\}, & \text{for } m = n, \\ \frac{1}{(k_m^2 - k_n^2) J_n} \left[h' \left\{ -k_n^2 U_n S_m + i\rho\omega^2 \left(\frac{k_m U_n U_m}{Z_{c,m}} - k_n Z_{c,n} V_n V_m \right) \right\} \right]_{-h}^h, & \text{for } m \neq n. \end{cases} \quad (D 2)$$

(a) *Biorthogonality condition*

Equation (A 5) applied to $\mathbf{Z}_1 = \mathbf{X}_n$ and $\mathbf{Z}_2 = \mathbf{Y}_m$ leads to

$$\begin{aligned} (\mathbf{F}\mathbf{G}\mathbf{X}_n | \mathbf{Y}_m) &= (\mathbf{X}_n | \mathbf{G}\mathbf{F}\mathbf{Y}_m) + ik_n [V_n R_m - R_n V_m]_{-h}^h \\ &+ ik_m [T_n U_m - U_n T_m]_{-h}^h. \end{aligned} \quad (D 3)$$

On the other hand, we also have $\mathbf{F}\mathbf{G}\mathbf{X}_n = -k_n^2 \mathbf{X}_n$ and $\mathbf{G}\mathbf{F}\mathbf{Y}_m = -k_m^2 \mathbf{Y}_m$. This leads to

$$(k_n^2 - k_m^2) (\mathbf{X}_n | \mathbf{Y}_m) = 0. \quad (D 4)$$

Our normalization for \mathbf{X}_n and \mathbf{Y}_n leads to

$$(\mathbf{X}_n | \mathbf{Y}_m) = J_n \delta_{nm}, \quad (D 5)$$

and its differentiated form

$$J'_n \delta_{nm} = (\partial_x \mathbf{X}_n | \mathbf{Y}_m) + (\mathbf{X}_n | \partial_x \mathbf{Y}_m) + [h' \mathbf{X}_n \mathbf{Y}_m]_{-h}^h. \quad (\text{D } 6)$$

References

- Abram, R. A. 1974 A coupled-mode formalism for elastic waveguides. *J. Phys. D: Appl. Phys.* **7**, 1329–1335. (doi:10.1088/0022-3727/7/10/305)
- Achenbach, J. D. 1987 *Wave propagation in elastic solids*, vol. II. Amsterdam/New York: North-Holland/Wiley.
- Besserer, H. & Malishewsky, P. G. 2004 Mode series expansions at vertical boundaries in elastic waveguides. *Wave Motion* **39**, 41–59. (doi:10.1016/S0165-2125(03)00069-6)
- Cho, Y. 2000 Estimation of ultrasonic guided wave mode conversion in a plate with thickness variation. *IEEE Trans. Ultrason. Ferro. Freq. Control* **47**, 591–603. (doi:10.1109/58.842046)
- Cho, Y. & Rose, J. L. 1996 A boundary element solution for a mode conversion study of the edge reflection of Lamb waves. *J. Acoust. Soc. Am.* **99**, 2097–2109. (doi:10.1121/1.415396)
- Folguera, A. & Harris, G. H. 1999 Coupled Rayleigh surface waves in a slowly varying elastic waveguide. *Proc. R. Soc. A* **455**, 917–931. (doi:10.1098/rspa.1999.0341)
- Fraser, W. B. 1976 Orthogonality relation for the Rayleigh–Lamb modes of vibration of a plate. *J. Acoust. Soc. Am.* **59**, 215–216. (doi:10.1121/1.380851)
- Galan, J. M. & Abascal, R. 2002 Numerical simulation of Lamb wave scattering in semi-infinite plates. *Int. J. Numer. Methods Eng.* **53**, 1145–1173.
- Galan, J. M. & Abascal, R. 2003 Elastodynamic guided wave scattering in infinite plates. *Int. J. Numer. Methods Eng.* **58**, 1091–1118.
- Galanenko, V. B. 1998 On coupled modes theory of two-dimensional wave motion in elastic waveguides with slowly varying parameters in curvilinear orthogonal coordinates. *J. Acoust. Soc. Am.* **103**, 1752–1762. (doi:10.1121/1.421330)
- Iserles, A., Marthinsen, A. & Norsett, S. P. 1999 On the implementation of the method of Magnus series for linear differential equations. *BIT* **39**, 281–304. (doi:10.1023/A:1022393913721)
- Karhitonov, A. V. 1978 Excitation of vibrations of an isotropic elastic strip by a system of volume and surface forces. *Sov. Phys. Acoust.* **24**, 339–343.
- Kennett, B. L. N. 1984 Guided wave propagation in laterally varying media—I. Theoretical development. *Geophys. J. R. Astr. Soc.* **79**, 235–255.
- Kirrmann, P. 1995 On the completeness of Lamb modes. *J. Elasticity* **37**, 39–69. (doi:10.1007/BF00043418)
- Koshiha, M., Karakida, S. & Suzuki, M. 1984 Finite-element analysis of Lamb wave scattering in an elastic plate waveguide. *IEEE Trans. Son. Ultrason.* **SU-311**, 18–25.
- Maupin, V. 1988 Surface waves across 2-D structures: a method based on coupled local modes. *Geophys. J.* **93**, 173–185.
- Murphy, J. E. & Li, G. 1994 Orthogonality relation for Rayleigh–Lamb modes of vibration of an arbitrarily layered elastic plate with and without fluid loading. *J. Acoust. Soc. Am.* **96**, 2313–2317. (doi:10.1121/1.410103)
- Pagneux, V. & Maurel, A. 2001 Determination of Lamb mode eigenvalues. *J. Acoust. Soc. Am.* **110**, 1307–1314. (doi:10.1121/1.1391248)
- Pagneux, V. & Maurel, A. 2002 Lamb wave propagation in inhomogeneous elastic waveguides. *Proc. R. Soc. A* **458**, 1913–1930. (doi:10.1098/rspa.2001.0950)
- Pagneux, V. & Maurel, A. 2004 Scattering matrix properties with evanescent modes for waveguides in fluids and solids. *J. Acoust. Soc. Am.* **116**, 1913–1920. (doi:10.1121/1.1786293)
- Pagneux, V., Amir, N. & Kergomard, J. 1996 A study of wave propagation in varying cross-section waveguides by modal decomposition. Part i. Theory and validation. *J. Acoust. Soc. Am.* **100**, 2034–2048. (doi:10.1121/1.417913)

- Perel, M. V., Kaplunov, J. D. & Rogerson, G. A. 2005 An asymptotic theory for internal reflection in weakly inhomogeneous elastic waveguides. *Wave Motion* **41**, 95–108. (doi:10.1016/j.wavemoti.2004.06.001)
- Press, W. H., Flannery, B. P., Teukolsky, S. A. & Vetterling, W. T. 1993 *Numerical recipes*. Cambridge: Cambridge University Press.
- Schiff, J. & Shnider, S. 1999 A natural approach to the numerical integration of Riccati differential equations. *SIAM J. Numer. Anal.* **36**, 1392–1413. (doi:10.1137/S0036142996307946)
- Tromp, J. 1994 A coupled local-mode analysis of surface-wave propagation in a laterally heterogeneous waveguide. *Geophys. J. Int.* **117**, 153–161.
- Viktorov, I. A. 1967 *Rayleigh and Lamb waves: physical theory and applications*, ch. 2. New York: Plenum Press.
- Wu, C., Duan, S. & Huang, Q. 2003 Effect of horizontal crack on Lamb wave propagation in a composite plate. *Key Eng. Mater.* **243**, 51–56.